ELSEVIER

Catalysis Today 78 (2003) 131–138

CATALYSIS TODAY

www.elsevier.com/locate/cattod

Catalytic activity and solid acidity of vanadium oxide thin layer loaded on TiO_2, ZrO_2, and SnO_2

Yuko Habuta, Naoaki Narishige, Kazu Okumura,
Naonobu Katada, Miki Niwa*

*Department of Materials Science, Faculty of Engineering, Tottori University,
Koyama, Tottori 680-8552, Japan*

Abstract

Vanadium oxide spread highly on TiO_2 (anatase, A) and SnO_2, and rather densely on TiO_2 (rutile, R) and ZrO_2 to make the monolayer in less than 4–5 V nm^{-2}. Profile of acid site of the monolayer was measured by temperature programmed desorption of ammonia, and its relation with the surface oxidation state was studied. The acid site density was high on the V_2O_5/TiO_2 (A) independent of the degree of oxidation. On the other hand, that of V_2O_5/TiO_2 (R) and V_2O_5/ZrO_2 depended on the oxidation state, and the high value of the concentration was observed on the oxidized one. The strength of acid site generated on the V_2O_5 monolayer on TiO_2 was as high as on the HZSM-5 zeolite. Turnover frequency (TOF) of propane conversion, and product selectivity were measured in propane oxidation. Among tested oxides, the V_2O_5/TiO_2 (A) showed the high TOF and selectivity to form propylene, while those loaded on TiO_2 (R) and ZrO_2 the small TOF and poor selectivity. Therefore, the reaction profile of activity and selectivity could be related with the extent of spreading and solid acidity. An idea of limit of the acid site density ca. 1.5 nm^{-2} on the monolayer was elucidated.

Keywords: Vanadium oxide monolayer; Solid acidity; Ammonia TPD; Propane oxidation; TiO_2; ZrO_2; SnO_2

1. Introduction

It has been recognized that the catalytic activity of metal oxide for oxidation reaction is often related with the solid acidity, although the role of the acid site is not well clarified. In our study on methanol oxidation [1,2], acidity was a prevailing parameter affecting the catalytic activity of the loaded molybdenum oxide. Methoxide intermediate to form formaldehyde seemed to be stabilized on the Brønsted acid site of the loaded molybdenum oxide monolayer, while the strongly stabilized intermediate on the bare support underwent the complete oxidation. This means that the acid site plays the role of stabilizing the selective reaction intermediate in the oxidation. Recently, much attention has been paid to the vanadium oxide catalysts for the selective oxidation of propane [3–11]. Our strategy in this field of investigation is directed to utilization of a simple structure of supported oxide, mono or thin layer, because it is relatively easy to characterize the surface, and correlate the obtained property with the catalytic activity and selectivity. In the present investigation, therefore, we will measure the solid acidity of the vanadium oxide thin layer on TiO_2, ZrO_2, and SnO_2, and the relationship with the catalytic activity and selectivity for propane oxidation into propylene will be studied.

---

* Corresponding author. Fax: +81-857-31-5256.
E-mail address: mikiniwa@chem.tottori-u.ac.jp (M. Niwa).

0920-5861/02/$ – see front matter © 2002 Elsevier Science B.V. All rights reserved.
PII: S0920-5861(02)00313-9

2. Experimental method

2.1. Catalysts

Ammonium metavanadate dissolved in water was reacted with oxalic acid to make the blue complex solution on a hot plate heated at 180 °C. Support metal oxide was put into the solution, followed by evaporation to dryness. Thus prepared vanadium-impregnated sample was calcined at 773 K for 3 h in a muffle oven.

Titania is reference catalyst, JRC-TIO3 (rutile phase, R) and JRC-TIO4 (anatase plus 10% rutile phase, A), both provided from Catalysis Society of Japan. ZrO_2 was prepared from $ZrO(NO_3)_2\cdot 2H_2O$ or available from Dai-ichi Kigenso, and shown as ZrO_2 (P) and (C), respectively. XRD of the samples showed that both of them contained monoclinic phase of ZrO_2 crystal principally. SnO_2 was prepared from a solution of $SnCl_2\cdot 2H_2O$, where it was dissolved into HCl solution followed by hydrolysis using ammonia water. The hydroxide gels thus obtained were dried and calcined in air at 773 K for 2 h.

2.2. Benzaldehyde ammonia titration

Spreading of the vanadium oxide on these supports was measured by a method of BAT (benzaldehyde–ammonia titration), where the selective adsorption of benzaldehyde on the support surface was experimentally proven. Details of the method by the usual pulse method were described previously [12].

2.3. Temperature programmed desorption of ammonia

Temperature programmed desorption (TPD) of ammonia was measured using a commercially available apparatus (Japan Bel, TPD-1-AT(NH_3)). About 0.1 g of the sample was evacuated at 773 K for 1 h, and then the bed temperature was cooled down to 373 K. Ammonia (1.33×10^4 Pa) was adsorbed, and then gaseous ammonia was evacuated. After the evacuation, water vapor (ca. 3×10^3 Pa) was admitted and evacuated at 373 K; the step of water vapor treatment was repeated twice. The bed temperature was elevated with a ramp rate of 10 K min^{-1}, and desorbed ammonia was detected by mass spectroscopy at 16 of m/e instead of 17, because of contamination by fragmentation of water. The sample was oxidized at 773 K with 760 Torr oxygen before adsorption of ammonia, when the influence by oxidation was studied.

2.4. Catalytic reaction

Catalytic activity was measured by a continuous flow method with a flow of 100 ml/min gas mixture containing $O_2/C_3H_8/N_2 = 15/15/70$. Products were analyzed using gas chromatography with columns of silicone and molecular sieves 13X for separation CO_2 and hydrocarbons, and O_2, N_2 and CO, respectively.

3. Results

3.1. Spreading of metal oxide on supports

Using a method of BAT, the extent of spreading of vanadium oxide on supports was measured. In Fig. 1, the coverage by vanadium oxide was plotted against the surface V atom concentration. Coverage on SnO_2 and TiO_2 (A) increased straightly with V atom concentration in less than 4–5 V nm^{-2}, and on further loading, it arrived at the saturated coverage of about 80%. On the other hand, on TiO_2 (R) and ZrO_2 (both P and C), the coverage increased in a smaller extent than on SnO_2 and TiO_2 (A) and arrived at the saturated coverage of about 70% in more than 5 V nm^{-2}. Thus, the spreading of vanadium oxide on these supports was found to be high on SnO_2 and TiO_2 (A), but rather low

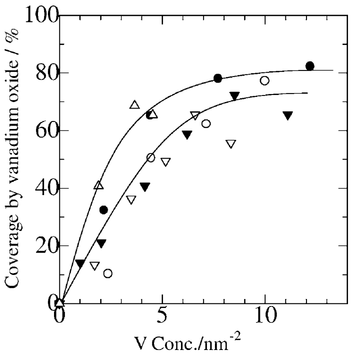

Fig. 1. Coverage by vanadium oxide on TiO_2 (A) (●), TiO_2 (R) (○), ZrO_2 (P) (▽), ZrO_2 (C) (▼), and SnO_2 (△) with increasing the V surface concentration.

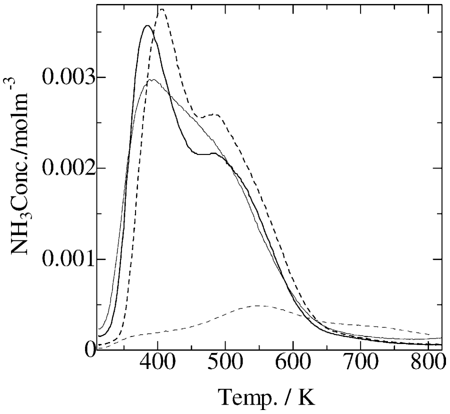

Fig. 2. TPD of ammonia on ZrO_2 (C) (thin) and V_2O_5 (8.51 V nm^{-2})/ZrO_2 (C) (thick) with (dotted) and without (solid) the water vapor treatment.

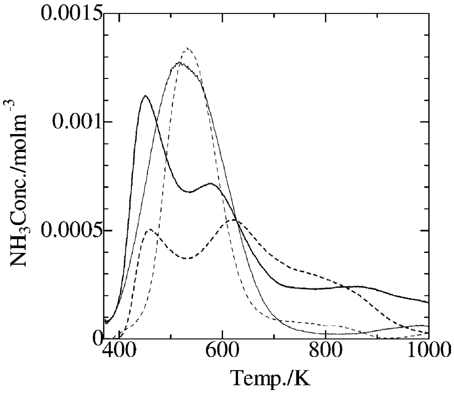

Fig. 3. TPD of ammonia on TiO_2 (A) (thin) and V_2O_5 (4.4 V nm^{-2})/TiO_2 (A) (thick) with (dotted) and without (solid) the water vapor treatment.

on TiO_2 (R) and ZrO_2 (both P and C). Highly spreading on the TiO_2 (A) has been observed previously at the similar surface concentration [13].

3.2. Solid acidity of the loaded vanadium oxide

In our previous investigation on MoO_3/SnO_2 [1] and WO_3/ZrO_2 [14], the water vapor treatment was utilized to measure the acid profile on the loaded metal oxide. The principle of method is a selective removal of ammonia adsorbed on the supports SnO_2 and ZrO_2, while almost no effect was observed on the loaded metal oxide. In this investigation, the water vapor treatment was examined on V_2O_5 on ZrO_2 (C) and TiO_2 (A). Fig. 2 shows the TPD profile measured by the experimental procedure with and without the water vapor treatment on V_2O_5/ZrO_2 and support ZrO_2 that were oxidized by 760 Torr O_2 prior to the experiment. As in previous investigations, admission of water vapor after adsorption of ammonia decreased the amount of desorbed ammonia on ZrO_2 significantly, whereas only the profile of desorption on the V_2O_5/ZrO_2 changed only a small extent. Thus, the treatment by water vapor was confirmed to be effective on the ZrO_2 support catalyst. However, the TPD profile on the V_2O_5 loaded on TiO_2 (A) and support in Fig. 3 showed a different effect, i.e., desorbed ammonia on TiO_2 (A) was not decreased, while the profile changed to some degree. On the V_2O_5/TiO_2 (A), however, not only amount but also profile of desorbed ammonia was not changed markedly. Therefore, the water vapor treatment is effective in removing ammonia adsorbed on ZrO_2 support, but not on TiO_2 support. The water vapor treatment was however undertaken throughout the present investigation, in order to compare all the experimental data at the same conditions. Some experimental errors were taken into account on the TiO_2 samples. Amount of loaded vanadium was adjusted to cover the surface of support as a monolayer exactly or in a little excess to that.

Figs. 4 and 5 show the effect by oxidation using oxygen at 773 K on V_2O_5 loaded on TiO_2 (A) and ZrO_2 (C), respectively. Oxidation of catalyst

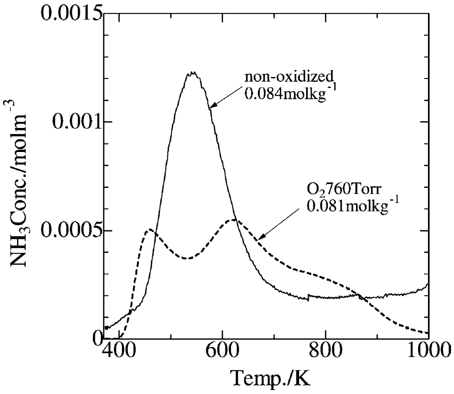

Fig. 4. TPD of ammonia on V_2O_5 (4.4 V nm^{-2})/TiO_2 (A) with (dotted) and without (solid) oxidation by 760 Torr O_2.

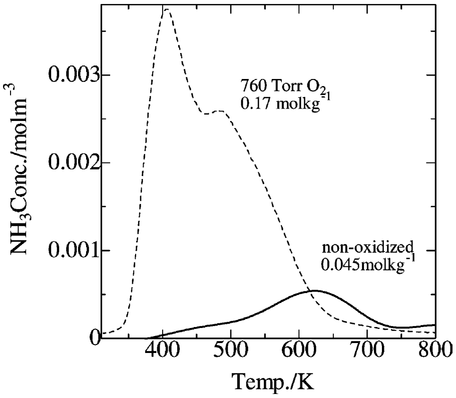

Fig. 5. TPD of ammonia on V_2O_5 (8.51 V nm^{-2})/ZrO_2 (C) with (dotted) and without (solid) oxidation by 760 Torr O_2.

using O_2 changed the profile of ammonia TPD on the V_2O_5/TiO_2 (A) (Fig. 4). Although the desorbed amount was changed in only a small extent, the desorption profile changed into two spikes pattern by 760 Torr O_2. This means that two kinds of acid site appeared by the oxidation. On the other hand, the desorbed amount was enhanced largely by oxidation on the V_2O_5/ZrO_2 (Fig. 5). Therefore, the TPD profile on the vanadium oxide loaded catalyst depended on the oxidation degree of surface, and qualitative and quantitative change was observed on TiO_2 (A) and ZrO_2, respectively.

In Table 1 listed are the amount and surface density of acid sites thus measured on the vanadium oxide loaded catalysts with 4–8 V nm^{-2} which corresponds to V atom surface density enough to cover the surface of support in a degree of 70–80%. V_2O_5/TiO_2 (A) showed the high concentration of acid site on both oxidized and non-oxidized conditions. The probability of acid site generation, i.e., surface density of acid site divided by loaded V atom, was ca. 1/4. This probability of acid site generation is often observed on the monolayer of metal oxide, such as WO_3 on ZrO_2 [14], MoO_3 on SnO_2 [1], etc. On the other hand, the amount of acid site on V_2O_5/TiO_2 (R) was small in the case without oxidation, but became large after oxidation by 760 Torr O_2. Concentration on V_2O_5/ZrO_2 (C) also depended upon the surface oxidation states, and high on the oxidized sample. V_2O_5/SnO_2 showed a relatively high concentration of acid site in both oxidized and non-oxidized conditions.

ΔH was measured from the TPD profile as a parameter of strength of acid site, on the basis of theory with freely re-adsorption of ammonia occurred [14]. So-called one-point method was used, where the value was calculated from the peak temperature and

Table 1
Profile of acid site measured by ammonia TPD with and without oxidation

Sample	Surface area ($m^2\,g^{-1}$)	V concentration (nm^{-2})	O_2 (Torr)	Acid site		
				Amount ($mol\,kg^{-1}$)	Density (nm^{-2})	ΔH ($kJ\,mol^{-1}$)
V_2O_5/TiO_2 (A)	47.1	4.4	760	0.081	1.04	152[a]
			0	0.084	1.1	133
V_2O_5/TiO_2 (R)	43.7	4.8	760	0.070	0.99	140
			0	0.023	0.31	142
V_2O_5/ZrO_2 (C)	69.7	8.51	760	0.172	1.49	114
			0	0.045	0.39	
V_2O_5/ZrO_2 (P)	50.1	5.16	0	0.030	0.36	
V_2O_5/SnO_2	23.5	4.53	760	0.052	1.33	
			0	0.058	1.50	
TiO_2 (A)	48.0	0	760	0.077	0.97	129
			0	0.084	1.1	136
TiO_2 (R)	44.1	0	760	0.037	0.47	132
			0	0.041	0.56	141
ZrO_2 (C)	82.0	0	0	0.020	0.15	
ZrO_2 (P)	45.0	0	0	0.014	0.19	
SnO_2	21.6	0	0	0.035	0.89	

[a] Only in this case, ΔH was measured from the desorption peak at a higher temperature.

experimental parameters.[1] As shown in Table 1, ΔH of the V_2O_5/TiO_2 (A) was 133–152 kJ mol^{-1}, and as large as on the ZSM-5 zeolite [15]. Such a high value of ΔH was obtained also on the V_2O_5/TiO_2 (R). On the other hand, the V_2O_5/ZrO_2 showed a little small value 114 kJ mol^{-1}.

Acidity of supports was also measured as a comparison, and shown in Table 1. Surface density of acid site was 1.0–0.9 nm^{-2} on TiO_2 (A) and SnO_2, 0.6 nm^{-2} on TiO_2 (R) and 0.2 nm^{-2} on ZrO_2. Oxidation of TiO_2 (A) and (R) decreased the acid site density in a small degree. ΔH on TiO_2 (A) and (R) was ca. 130–140 kJ mol^{-1}, and it was a little larger on the TiO_2 (R).

3.3. Infrared spectra of adsorbed ammonia

As shown in Fig. 6, an absorption was observed at 1600 cm^{-1} on oxidized TiO_2 (A), and was identified as NH_3 adsorbed on Lewis acid site. Intensity of this band was not decreased strongly by the water vapor treatment. Bands at 1380 and 1358 cm^{-1} were observed, but not fully identified. On the other hand, two kinds of absorption were observed on the V_2O_5/TiO_2 (A) at 1420 and 1600 cm^{-1}, which were ascribable to ammonia molecules on Brønsted and Lewis acid sites, respectively (Fig. 7). These absorptions were decreased upon evacuation at 573–673 K. As shown in Fig. 7f, the infrared spectrum on the oxidized sample was not different from un-oxidized one in Fig. 7b. Therefore, the change of TPD profile by oxidation with 760 Torr O_2 was not clarified by infrared spectroscopy. The present findings for the identification of Brønsted and Lewis acid site were in agreement with those of previous study [16], and it was confirmed that ammonia was adsorbed on the loaded V_2O_5 and TiO_2 support as ammonium cation and coordinately adsorbed ammonia, respectively.

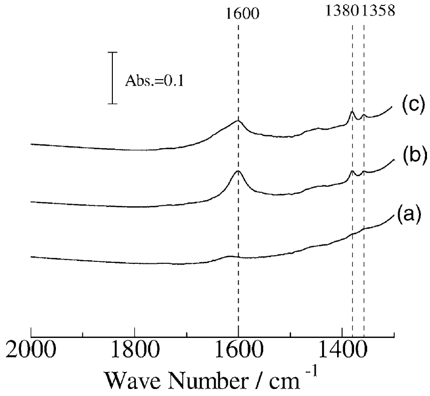

Fig. 6. Infrared spectra of TiO_2 (A) after evacuated at 773 K (a), followed by adsorption of ammonia (b) and the water vapor treatment at 373 K (c).

3.4. Catalytic activity of propane oxidation

Catalytic activity was measured at temperatures 573–773 K. Oxidation of propane yielded CO, CO_2 and propylene. Fig. 8 shows the change of products yield and propane conversion with the loaded

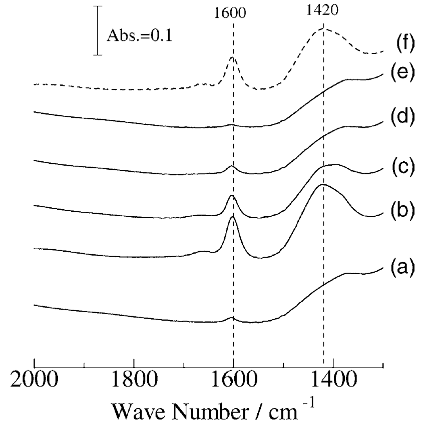

Fig. 7. Infrared spectra of V_2O_5 (4.4 V nm^{-2})/TiO_2 (A) after evacuated at 773 K (a), followed by adsorption of ammonia at 373 K (b), and subsequent evacuation at 473 K (c), 573 K (d), and 673 K (e). Experimental run (f) was obtained after oxidation with 760 Torr O_2, followed by adsorption of ammonia and evacuation at 373 K for a comparison.

---

[1] $\ln T_m - \ln(A_0 W/F) = (\Delta H/RT_m) + \ln(\beta(1-\theta_m)^2(\Delta H - RT_m)/P^0 \exp(\Delta S/R))$, where R is the gas constant (8.314 J K^{-1} mol^{-1}), T_m the temperature at desorption peak (K), β the heating rate (K s^{-1}), θ_m the coverage of the acid site by ammonia at the peak maximum, P^0 the pressure at standard conditions (1.013×10^5 Pa), ΔH the adsorption heat of ammonia (J mol^{-1}), and ΔS the entropy change with respect to the desorption of ammonia. A_0, W, and F are amount of acid site (mol kg^{-1}), flow rate of carrier gas (m^3 s^{-1}) and weight of the sample (kg), respectively. Parameters except for ΔH and ΔS are provided from experiment. ΔS consists of ΔS (mixing) and ΔS (phase transformation), ΔS (mixing) is calculated from mole fractions of ammonia and carrier gas helium, and ΔS (phase transformation) is assumed to be 95 J K^{-1} mol^{-1} that is close to ΔS for liquid ammonia vaporization.

Table 2
TOF, conversion of propane, and selectivity to form propylene at 723 K

Sample[a]	Surface concentration ($V\,nm^{-2}$)	TOF for propane[b] conversion (s^{-1})	Conversion of propane (%)	Selectivity to propylene (%)
V_2O_5/TiO_2 (A)	4.4	0.12	11.6	43.3
V_2O_5/TiO_2 (R)	4.8	0.066	6.9	30.5
V_2O_5/ZrO_2 (P)	5.2	0.033	21.3	25.8
V_2O_5/ZrO_2 (C)	4.2	0.028	21.2	23.4
V_2O_5/SnO_2	4.5	0.47	8.2	0.8

[a] 0.03 and 0.15 g of TiO_2 and other supports loaded catalyst, respectively, was used.
[b] On the basis of the loaded vanadium atom.

vanadium concentration on V_2O_5/TiO_2 (A) at 723 K. The yield of propylene showed the maximum at 4–5 $V\,nm^{-2}$ where the coverage arrived at the saturated degree of 80%. On further loading, propylene yield decreased at the expense of CO and CO_2 formation. This means that the monolayer has the selective activity to form propylene, while the thick layer with excess amount of vanadium does not. Turnover frequency (TOF) for propylene formation at 723 K was calculated in order to compare the activities as shown in Table 2. The V_2O_5 loaded on TiO_2 (A) showed higher TOF than TiO_2 (R) and ZrO_2. In addition, TiO_2 (A) is the support to show the highest selective activity to produce propylene, but TiO_2 (R) and ZrO_2 make the vanadium oxide less selective, as shown in Table 2.

V_2O_5/SnO_2 showed the high TOF with non-selective activity to produce a large amount of CO and CO_2 preferentially. Combustion occurred in a high degree even on the support SnO_2 itself.

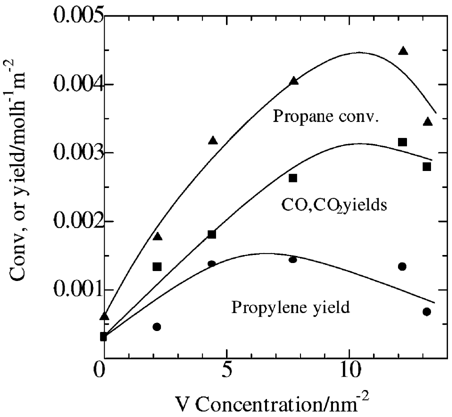

Fig. 8. Propane oxidation at 723 K on V_2O_5/TiO_2 (A) by varying the V concentration.

4. Discussion

4.1. Structure of loaded vanadium oxide

From the BAT measurements, the extent of coverage by vanadium oxide was measured, and the behavior of vanadium oxide spreading on supports could be estimated. Obviously, the vanadium oxide spreads more readily on TiO_2 (A) and SnO_2 than on TiO_2 (R) and ZrO_2. Therefore, different structures of the loaded vanadium oxide are speculated on these supports. However, on these supports, the coverage increased almost linearly with the surface concentration of vanadium until it arrived at the saturated conditions. Thus, it is suggested that the vanadium oxide spreads on these supports with a structure of monolayer, and the structure depends on the kind of support. Extrapolation of linear plots between coverage and surface vanadium atom concentration arrives at 100% in ca. 4.5 and 8 $V\,nm^{-2}$, on TiO_2 (A) and SnO_2, and TiO_2 (R) and ZrO_2, respectively. Exposed vanadium atom on the surface of V_2O_5 crystal occupies surface area of 0.16–0.25 nm^2, and therefore 3.9–6.4 V atom/nm^2 could be exposed onto the surface of the loaded vanadium oxide.[2] The experimental findings in this investigation are within this range of vanadium atom density on the exposed surface. Therefore, vanadium oxide on all the supports studied in this investigation spreads as the monolayer, as long as the surface concentration is smaller than 4–5 $V\,nm^{-2}$.

When the extent of spreading is compared with the solid acidity of support, we may indicate that the high spreading is obtained on the metal oxide

---

[2] V_2O_5 crystal has the dimension (*a*, *b*, *c*; 1.152, 0.356, 0.437 nm) and *Z*: 2.

with the high acid site density. Because the *acidic* vanadium oxide spreads on the *basic* support, the basicity of metal oxide would influence on the extent of spreading. However, the acid site measured on the supports is characteristic of Lewis type; therefore, the combination of Lewis acid and base center due to the coordination unsaturated site is created by the dehydration. Therefore, the high concentration of acid site, on the other hand, indicates the high concentration of base site in equal probability. Therefore, it is rationally proven that the high spreading is realized on the support with the high concentration of acid site.

4.2. Generation of acid site on the monolayer

Generation of acid site on the monolayer metal oxide is most probably due to the interaction between metal oxide and support. As previously stated [17], the driving force of metal oxide spreading is an interfacial interaction between oxide and support, and acidic oxide plays the role of electron acceptor from a donor base material. Therefore, the more is the difference in properties of metal oxide and support, the more the loaded metal oxide spread. SO_4^{2-}, WO_3, MoO_3, and V_2O_5 are acidic metal oxides and spread readily on the basic oxide support such as SnO_2, ZrO_2, TiO_2, and Al_2O_3. On the other hand, there are many binary metal oxide combinations between them to show the strong solid acidity. SO_4^{2-}, WO_3, and MoO_3 loaded on SnO_2 and ZrO_2 are typical combinations to show the strong acidity. However, V_2O_5 showed the strong acidity of 133–152 $kJ\,mol^{-1}$ of ammonia desorption upon loading on TiO_2 (both A and R), but only 110 $kJ\,mol^{-1}$ on ZrO_2. Strong acid site is therefore created, dependent on kinds of loaded metal oxide and support.

TiO_2 (A) makes vanadium oxide to show not only the highest spreading but also the large acid site concentration. The generation probability of acid site ca. 1/4–1/5 against loaded atom is often obtained on the monolayer, as mentioned above. However, up to now, the generation probability has not been elucidated. We want to propose an idea of the limit in surface acid site density to prove it, on the basis of information about the zeolite acidity. In the proton type zeolite exposed to usual atmosphere, 1.5 mol/kg on the H-mordenite with 15 of Si/Al_2 ratio is the maximum concentration, and larger than on other type zeolites with any composition [18]. The surface area of the mordenite being about 400 $m^2\,g^{-1}$, 2.0 nm^{-2} is the maximum surface acid site density. When the site density exceeds this value, acid sites destroy partially due to the mutual interaction. The self-destruction of acid site occurs only on the zeolite with a high concentration, as observed in the proton type Y and mordenite [19]. Mechanism of the self-destruction has not been clarified, although, most probably, water may have a key role. This idea of limit in acid site density can explain the acid site concentration on metal oxide. The acid site density 1.1–1.5 nm^{-2} on the loaded V_2O_5 on TiO_2 and ZrO_2 with and without oxidation is close to the maximum density on the zeolite. The acid site is generated on four to five metal atoms on the monolayer at the coverage of 70–80%. In other words, four to five metal atoms are required *usually* to cover the support surface as the monolayer, and the acid site density is limited to ca. 1.5–2 nm^{-2}; thus, the generation probability may become 1/4–1/5.

4.3. Catalytic activity in propane oxidation

Oxidation of propane occurs on the vanadium oxide and therefore requires the high oxidation ability. In this study, relatively reducing conditions of reactant mixture are used; therefore, the surface of metal oxide is subjected to the reduction during the reaction. As revealed by the TPD of ammonia, V_2O_5/ZrO_2 seems to be easily reduced only by the evacuation, because the TPD profile changed strongly after the oxidation. On the other hand, V_2O_5/TiO_2 (A) is kept at the highly oxidized conditions, because the number of acid sites is not changed. When the reduced sites are created on the surface, hydrocarbon and oxygen-containing residue are stabilized, and the adsorbed species finally undergoes the combustion into CO and CO_2. In order to enhance the selective oxidation, thereby, highly oxidized conditions may be required. The acid site thus kept on the surface can accommodate an intermediate species to form the selective product. V_2O_5/TiO_2 (A) may have this property to realize the selective activity in propane oxidation. On the other hand, V_2O_5 on TiO_2 (R) and ZrO_2 showed the high acid site density only on the conditions after oxidation by O_2 760 Torr. Maybe, vanadium oxide on these supports is reduced in some degree during the reaction, where the oxidation reaction proceeds non-selectivity. Thereby, keeping the high oxidation state during the reaction is an important property of the V_2O_5/TiO_2 (A) which enables the selective oxidation reaction.

However, conditions on the V_2O_5/SnO_2 seem to be different from other catalysts, because non-selective reaction occurs preferentially in spite of the high concentration of acid site. Previous investigations showed that tin atom was mixed into the vanadium surface to enhance the oxygen mobility [20]. The surface conditions may be adequate for selective oxidation and ammoxidation of aromatic compounds [21]. However, it seems to be not available for selective oxidation of paraffin.

5. Conclusions

1. The selective activity of the V_2O_5 on TiO_2 (A) for oxidation of propane is caused by the high concentration of acid site independent of the oxidation conditions.
2. The strength of acid site on the V_2O_5 on TiO_2 (A) is as high as on zeolite ZSM-5.
3. Generation probability of acid site on the metal oxide monolayer is explained from the limit of acid site density.

References

[1] M. Niwa, J. Igarashi, Catal. Today 52 (1999) 71.
[2] N. Narishige, M. Niwa, Catal. Lett. 71 (2001) 63.
[3] A. Adamski, Z. Sojka, K. Dyrek, M. Che, G. Wendt, S. Albrecht, Langmuir 15 (1999) 5733.
[4] J.M.L. Nieto, J. Soler, P. Concepcion, J. Herguido, M. Menendez, J. Santamaria, J. Catal. 185 (1999) 324.
[5] V. Ermini, E. Finocchio, S. Sechi, G. Busca, S. Rossini, Appl. Catal. A 198 (2000) 67.
[6] R.X. Valenzuela, V.C. Corberan, Top. Catal. 11 (2000) 153.
[7] T. Ono, Y. Tanaka, T. Takeuchi, K. Yamamoto, J. Mol. Catal. A 159 (2000) 293.
[8] A.A. Lemonidou, L. Nalbandian, L.A. Vasalos, Catal. Today 61 (2000) 333.
[9] Y. Wang, Q.H. Zhang, Y. Ohishi, T. Shishido, K. Takehira, Catal. Lett. 72 (2001) 215.
[10] P. Rybarczyk, H. Berndt, J. Radnik, M.M. Pohl, O. Buyevskaya, M. Baerns, A. Bruckner, J. Catal. 202 (2001) 45.
[11] B. Solsona, T. Blasco, J.M.L. Nieto, M.L. Pena, F. Rey, A. Vidal Moya, J. Catal. 203 (2001) 443.
[12] M. Niwa, S. Inagaki, Y. Murakami, J. Phys. Chem. 89 (1985) 3869.
[13] I.E. Wachs, R.Y. Saleh, S.S. Chan, C.C. Chersich, Appl. Catal. 15 (1985) 339.
[14] N. Naito, N. Katada, M. Niwa, J. Phys. Chem. B 103 (1999) 7206.
[15] N. Katada, H. Igi, J.H. Kim, M. Niwa, J. Phys. Chem. B 101 (1997) 5969.
[16] M. Inomata, K. Mori, A. Miyamoto, T. Ui, Y. Murakami, J. Phys. Chem. 87 (1983) 754.
[17] M. Niwa, Y. Matsuoka, Y. Murakami, J. Phys. Chem. 91 (1987) 4519.
[18] M. Sawa, M. Niwa, Y. Murakami, Zeolite 10 (1990) 532.
[19] N. Katada, Y. Kageyama, M. Niwa, J. Phys. Chem. B 104 (2000) 7561.
[20] F. Okada, A. Satsuma, A. Furuta, A. Miyamoto, T. Hattori, Y. Murakami, J. Phys. Chem. 94 (1990) 5900.
[21] L.T. Andersson, S. Jaras, J. Catal. 64 (1980) 51.